IET Communications

Research Article

Interpolation based pilot-aided channel estimation for STBC spatial modulation and performance analysis under imperfect CSI

ISSN 1751-8628
Received on 5th February 2016
Revised on 12th April 2016
Accepted on 21st May 2016
doi: 10.1049/iet-com.2016.0151
www.ietdl.org

Yusuf Acar[1] ✉, Hakan Doğan[2], Ertuğrul Başar[3], Erdal Panayirci[4]

[1]Department of Electrical and Electronics Engineering, Istanbul Kultur University, 34156, Bakirkoy, Istanbul, Turkey
[2]Department of Electrical and Electronics Engineering, Istanbul University, 34320, Avcilar, Istanbul, Turkey
[3]Faculty of Electrical and Electronics Engineering, Istanbul Technical University, 34469, Maslak, Istanbul, Turkey
[4]Department of Electrical and Electronics Engineering, Kadir Has University, 34083, Istanbul, Turkey
✉ E-mail: y.acar@iku.edu.tr

Abstract: A combination of space-time block coding and spatial modulation (STBC-SM) has been recently proposed for multiple input-multiple output systems to obtain both spatial diversity gain and more capacity simultaneously while assuming the perfect channel state information (P-CSI) was available at the receiver. However, in practical scenarios the CSI is unknown to the receiver and should be estimated in order to detect the transmitted data in a reliable way. Therefore, channel estimation (CE) is a major challenge in designing the STBC-SM systems. In this study, the problem of CE is investigated and a new pilot-aided channel estimation (PA-CE) technique, coupled with an interpolation, is proposed for the STBC-SM systems operating in the presence of rapidly time-varying mobile channels. Several interpolation schemes such as the linear, nearest neighbour, piecewise cubic Hermite and the low-pass interpolations are applied and their performances are compared to determine the best suitable interpolation technique to be employed in STBC-SM systems. Bit error rate (BER) performance of the proposed CE technique is then investigated in time-varying channels with different modulation. Moreover, the pairwise error probability of the STBC-SM scheme is derived and its average bit error probability is evaluated analytically in the presence of CE errors.

1 Introduction

Multiple-antenna techniques constitute a key technology, creating multiple independent channels for sending multiple data streams [1]. Inter channel interference and inter antenna synchronisation are traditional problems associated with practical multiple-input and multiple-output (MIMO) systems. To circumvent these problems, spatial modulation (SM) was proposed by Mesleh *et al.* [2] as a low complexity alternative to conventional MIMO transmission schemes.

Space time block coding (STBC) and in particular Alamouti's STBC scheme [3] takes advantage of a space diversity in MIMO systems. Recently, SM and STBC have been combined to benefit the advantages of both systems while avoiding their drawbacks [4] and shown that the STBC-SM scheme, in which the information is transferred with an STBC matrix and active transmit antenna indices, had superior performance and simple implementation as compared with the SM systems, due to its diversity advantage and smaller number of transmit antennas employed. As a result, the STBC based SM exploits the space, time and antenna domains to transmit information bits while it benefits from the diversity gain of the STBC scheme.

To the best of our knowledge, all of the STBC-SM works in the literature have assumed that the perfect channel state information (P-CSI) was available at the receiver. Despite the fact that it is impossible to obtain the P-CSI for practical systems, the accuracy of the channel estimation (CE) is very critical for the operation the pilot assisted channel estimation (PA-CE). PA-CE with interpolation is one of the promising and preferred techniques for time-varying channels because of its robustness against several imperfections during detection at the receiver as well as its simple implementation and superior performance. The CE coupled with interpolation techniques is widely adapted in current communication systems and proposed for new wireless systems, such as IEEE 802.16m worldwide interoperability for microwave access [5], the third generation partnership project and long-term evolution advanced [6]. Therefore, interpolation techniques such as nearest interpolation (NI), piecewise linear interpolation (PLI) and low-pass interpolation (LPI) can be adopted to solve the CE problem in real applications. In [7], interpolation based CE techniques for orthogonal frequency division multiplexing systems were proposed. Linear, low-pass, spline cubic and time domain interpolation techniques have been also investigated and it was shown that the comb-type PA-CE with LPI performed the best among all these CE algorithms [7].

In this paper, a new PA-CE technique is proposed for STBC-SM systems in which a training sequence consisting of known data symbols (pilots) are employed in each transmitted frame. Note that, as explained shortly, designing a PA-CE algorithm for the STBC-SM systems, particularly in the presence of rapidly varying channels, is quite different and challenging than the conventional PA-CE techniques due to the special structure of the STBC-SM scheme since the interpolation technique employed in the CE algorithm should satisfy some specific requirements. It is known and demonstrated that the PA-CE methods are computationally simple, effective as well as efficient and the channel impulse response (CIR) at the pilot positions can be easily estimated by using a least squares (LS) estimation technique. After that, the fast fading channel coefficients are estimated by interpolation at time instants at which data symbols are transmitted. The variations in fast fading coefficients are tracked in this way in an efficient manner. Thus, our investigations in this paper on PA-CE for the STBC-SM systems are also focused on several efficient interpolation techniques such as the LPI, PLI, NI, spline interpolation (SI), pchip interpolation (PI) techniques.

Moreover, the pairwise error probability (PEP) of STBC-SM is derived analytically in this paper for general M-ary signal constellations and the average bit error probability (ABEP) of

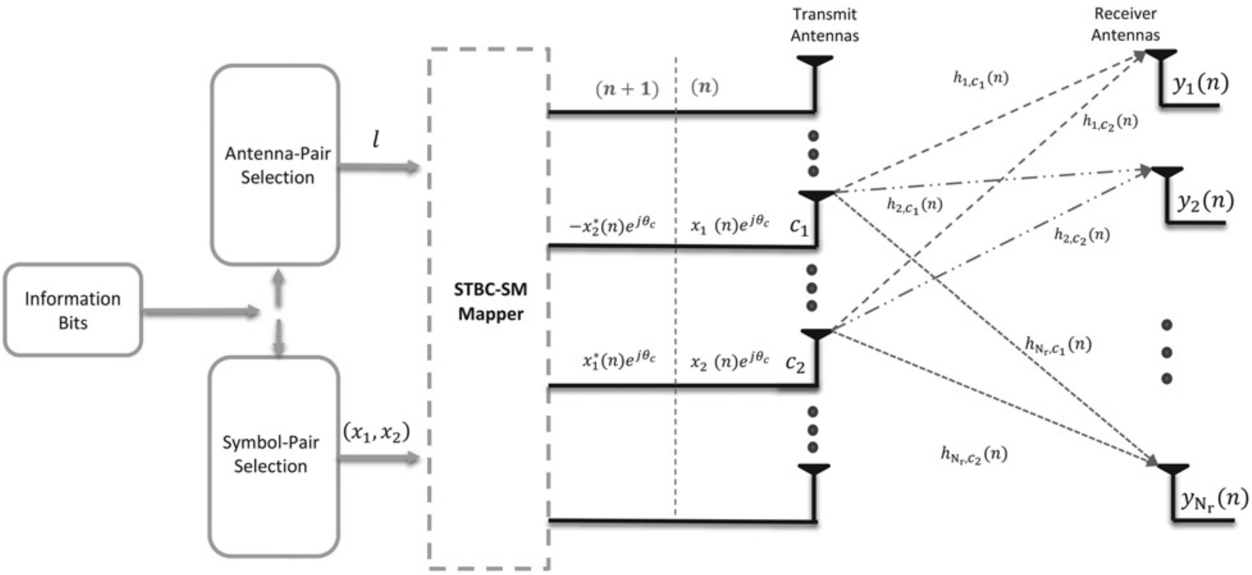

Fig. 1 *Transmitter block diagram for the STBC-SM system*

STBC-SM is evaluated in the presence of CE errors. Computer simulations indicate that the derived theoretical curves become very tight with increasing signal to noise ratio (SNR) for the STBC-SM systems.

Notation: Throughout the paper, the following notations and assumptions are used. Bold and capital letters '$\boldsymbol{A}$' denote matrices. Bold and small letters '$\boldsymbol{a}$' denote vectors. The notations, $(.)^*$, $(.)^T$, $(.)^\dagger$, $(.)^{-1}$, $\|.\|$ and $\|.\|_F$ denote conjugate, transpose, Hermitian, inverse, Euclidean norm and Frobenius norm of a matrix or a vector, respectively. $\mathbb{C}$ represents the ring of complex numbers. For complex variable x, $\Re\{x\}$ denote the real part of x. $\mathcal{CN}(0, \sigma^2)$ is circularly symmetrical Gaussian distribution with variance σ^2. $Q(.)$ is tail probability of the standard Gaussian distribution. The PDF of the r.v. x denoted by $p_X(x)$.

2 Space–time block coded spatial modulation

In this paper, we consider the STBC-SM technique with a Alamouti's scheme as the core STBC introduced in [4] and in some other studies in the literature [8, 9]. Let us consider an $N_t \times N_r$ STBC-SM system employing the Alamouti's STBC with C pairs of transmit antennas where N_t and N_r are the number of transmit and receive antennas, respectively. The total number of possible pairs is selected as

$$C = \left\lfloor \binom{N_t}{2} \right\rfloor_{2^p},$$

where p is a positive integer and $\lfloor x \rfloor_{2^p}$ shows the largest integer less than or equal to x that is an integer power of 2. Fig. 1 shows the transmitter block diagram of an STBC-SM system where information bits are mapped into transmitted symbols according to the modulation format employed and the corresponding antenna pair during each two consecutive symbol intervals. The first $\log_2 C$ bits determine the antenna-pair position and the symbol pair is determined by the last $2\log_2 M$ bits where M is the modulation order.

In the STBC system, two complex symbols (x_1 and x_2), selected from an M-QAM or M-PSK constellation, are transmitted from two transmit antennas in two symbol consecutive intervals [3]. For the STBC-SM scheme, the STBC code matrix is extended to the antenna domain, consisting of N_t transmit antennas, in such a way that both the indices of the transmit antennas from which these symbols are transmitted and STBC symbols, convey information, as follows. First, a pair of transmit antennas $c = (c_i, c_j) \in \{1, 2, \ldots, N_t\}$, $(c_i \neq c_j)$ with a label $\ell \in \{1, 2, \ldots\}$ is chosen. For instance, the total number of possible pairs for four transmit antennas case is six and a maximum two bits per label can be transmitted by selecting any of the four possible antenna-pair combinations. In the first symbol interval, the transmission vector of the STBC-SM system can be defined as

$$\boldsymbol{x}_c^1(n) = [0\ 0 \ldots \overbrace{x_1(n)\psi_c}^{c_1\text{th}} \ldots \overbrace{x_2(n)\psi_c}^{c_2\text{th}} \ldots 0] \tag{1}$$

where $\psi_c \triangleq e^{j\theta_c}$, θ_c is a rotation angle, n is discrete time index, c_1th and c_2th elements of $\boldsymbol{x}_c^1(n)$ show the two active antennas of Cth pair of transmit antennas. The transmission vector within the second symbol interval for the STBC-SM system can be written as

$$\boldsymbol{x}_c^2(n+1) = [0\ 0 \ldots \overbrace{-(x_2^*(n)\psi_c)}^{c_1\text{th}} \ldots \overbrace{(x_1^*(n)\psi_c)}^{c_2\text{th}} \ldots 0] \tag{2}$$

where $\boldsymbol{x}_c^1(n)$ and $\boldsymbol{x}_c^2(n+1)$ are $1 \times N_t$ dimensional signal vectors. In [4], the parameters ℓ, $c = (c_1, c_2)$ and the optimal rotation angles θ_c are given for QPSK, 16-QAM and 64-QAM signal constellations.

For the STBC-SM scheme only two transmit antennas are active during one symbol interval and the other antennas remain silent over this interval. Therefore, signal vectors of (1) and (2) have $N_t - 2$ zeros entries. After the mapping process, the signal matrix $\boldsymbol{X} = [\boldsymbol{x}_c^1\ ;\ \boldsymbol{x}_c^2]$, $c \in [1:C]$ is transmitted over an $N_t \times N_r$ MIMO channel.

We can express the received signals obtained at the output of each receive antenna $r = 1, \ldots, N_r$ in two consecutive discrete-time intervals n and $n+1$ as follows

$$\begin{aligned} y_r(n) &= h_{r,c_1}(n)\psi_c x_1(n) + h_{r,c_2}(n)\psi_c x_2(n) + w_r(n) \\ y_r(n+1) &= -h_{r,c_1}(n+1)\psi_c x_2^*(n) \\ &\quad + h_{r,c_2}(n+1)\psi_c x_1^*(n) + w_r(n+1) \end{aligned} \tag{3}$$

where $h_{r,c_i}(n)$ is a channel coefficient between the transmit antenna $c_i \in \{1, 2, \ldots, C\}$ and rth receiver antenna. $w_r(n)$ is a complex-valued, zero-mean additive white Gaussian noise with variance σ_w^2. From (3),

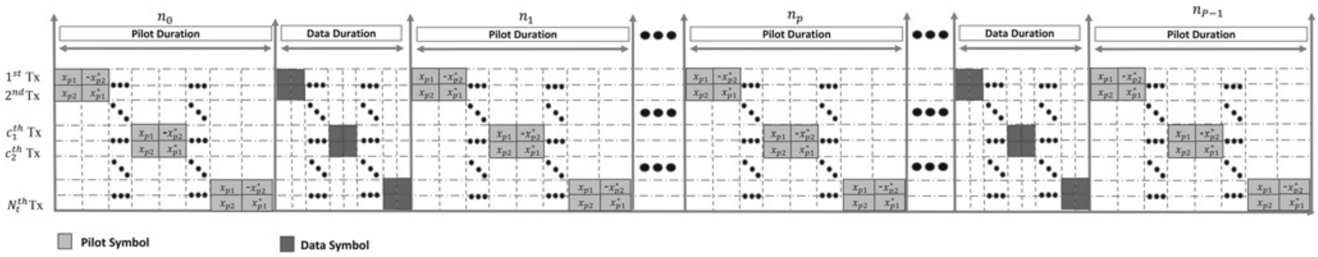

Fig. 2 *Frame structure, n_p, $p = 0, 1, 2, \ldots, P-1$ denotes pilot durations and x_{p_i}, $i = 1,2$ denotes pilot symbols*

the received signals can be written in the matrix form as follows

$$\begin{bmatrix} y_1(n) \\ y_1^*(n+1) \\ y_2(n) \\ y_2^*(n+1) \\ \vdots \\ y_{N_r}(n) \\ y_{N_r}^*(n+1) \end{bmatrix} = \begin{bmatrix} h_{1,c_1}(n)\psi_c & h_{1,c_2}(n)\psi_c \\ h_{1,c_2}^*(n+1)\psi_c^* & -h_{1,c_1}^*(n+1)\psi_c^* \\ h_{2,c_1}(n)\psi_c & h_{2,c_2}(n)\psi_c \\ h_{2,c_2}^*(n+1)\psi_c^* & -h_{2,c_1}^*(n+1)\psi_c^* \\ \vdots & \vdots \\ h_{N_r,c_1}(n)\psi_c & h_{N_r,c_2}(n)\psi_c \\ h_{N_r,c_2}^*(n+1)\psi_c^* & -h_{N_r,c_1}^*(n+1)\psi_c^* \end{bmatrix} \begin{bmatrix} x_1(n) \\ x_2(n) \end{bmatrix} + \begin{bmatrix} w_1(n) \\ w_1^*(n+1) \\ w_2(n) \\ w_2^*(n+1) \\ \vdots \\ w_{N_r}(n) \\ w_{N_r}^*(n+1) \end{bmatrix}. \quad (4)$$

Under the assumption that the time-varying Rayleigh distributed channel coefficients between jth transmitter antenna and rth receiver antenna do not change over these two time intervals, that is, $h_{r,j}(n+1) \simeq h_{r,j}(n)$, the following equivalent observation model can be obtained from (3), for $\ell \Leftrightarrow c = (c_1, c_2)$, in a vector form

$$\boldsymbol{y}(n) = \mathrm{diag}(\psi_l)\boldsymbol{H}_\ell \begin{bmatrix} x_1(n) \\ x_2(n) \end{bmatrix} + \boldsymbol{w}(n) \quad (5)$$

where $\boldsymbol{H}_\ell(n) = [\boldsymbol{h}_\ell^{(1)}(n)\ \boldsymbol{h}_\ell^{(2)}(n)]$, $\boldsymbol{h}_\ell^{(1)}(n) = \big[h_{1,c_1}(n) \quad h_{1,c_2}^*(n) \quad h_{2,c_1}(n) \quad h_{2,c_2}^*(n) \quad \cdots \quad h_{N_r,c_1}(n) \quad h_{N_r,c_2}^*(n)\big]^{\mathrm{T}}$, $\boldsymbol{h}_\ell^{(2)}(n) = \big[h_{1,c_2}(n) \quad -h_{1,c_1}^*(n) \quad h_{2,c_2}(n) \quad -h_{2,c_1}^*(n) \quad \cdots \quad h_{N_r,c_2}(n) \quad -h_{N_r,c_1}^*(n)\big]^{\mathrm{T}}$ and $\boldsymbol{\psi}_l = [\psi_c, \psi_c^*, \psi_c, \psi_c^*, \ldots, \psi_c, \psi_c^*]^{\mathrm{T}}$.

3 Detection in STBC-SM systems

The STBC-SM receiver with the ML detector is considered where $\widehat{\boldsymbol{H}}_l(n)$ is the estimate of $\boldsymbol{H}_l(n)$. There are C equivalent channel matrices $\boldsymbol{H}_\ell$, $0 \le \ell \le C-1$ in total, and for the ℓth combination, the receiver calculates the ML estimates of x_1 and x_2 by the use of the orthogonality of $\boldsymbol{h}_\ell^{(1)}(n)$ and $\boldsymbol{h}_\ell^{(2)}(n)$

$$\begin{aligned} \hat{x}_{1,\ell}(n) &= \arg\min_{x_1} \left\| \boldsymbol{y}(n) - \mathrm{diag}(\boldsymbol{\psi}_l)\boldsymbol{h}_\ell^{(1)}(n)x_1 \right\|^2 \\ \hat{x}_{2,\ell}(n) &= \arg\min_{x_2} \left\| \boldsymbol{y}(n) - \mathrm{diag}(\boldsymbol{\psi}_l)\boldsymbol{h}_\ell^{(2)}(n)x_2 \right\|^2. \end{aligned} \quad (6)$$

To calculate the total ML metric for ℓth combination, minimum ML metrics $m_{1,\ell}(n)$ and $m_{2,\ell}(n)$ for x_1 and x_2 are calculated as

$$\begin{aligned} m_{1,\ell}(n) &= \min_{x_1} \left\| \boldsymbol{y}(n) - \mathrm{diag}(\boldsymbol{\psi}_l)\boldsymbol{h}_\ell^{(1)}(n)x_1 \right\|^2 \\ m_{2,\ell}(n) &= \min_{x_2} \left\| \boldsymbol{y}(n) - \mathrm{diag}(\boldsymbol{\psi}_l)\boldsymbol{h}_\ell^{(2)}(n)x_2 \right\|^2, \end{aligned} \quad (7)$$

respectively. Then their summation $m_\ell(n) = m_{1,\ell}(n) + m_{2,\ell}(n)$ provides the total ML metric for $0 \le \ell \le C-1$. Finally, a decision has been made by selecting the minimum antenna combination metric as $\hat{\ell}(n) = \arg\min_\ell m_\ell(n)$ for which $(\widehat{x}_1(n), \widehat{x}_2(n)) = (\widehat{x}_{1,\widehat{\ell}}(n), \widehat{x}_{2,\widehat{\ell}}(n))$.

4 Channel estimation for the STBC-SM system

In an $N_t \times N_r$ STBC-SM system, CSI is needed to detect the modulated symbols, $(\widehat{x}_1(n), \widehat{x}_2(n))$, and the transmit antenna pair number, $\widehat{l}(n)$. Generally, most of the studies on CE assume a slow fading channel. However, in practice, wireless systems may operate in the presence of time-varying channels caused by high mobility, resulting in rapid fluctuations in the fading channel coefficients.

In this section, we propose an efficient and low complexity CE technique suitable for the STBC-SM systems which is implemented in two steps. As shown in Fig. 2, in the first step, the channel coefficients are estimated at the positions of the pilots, n_p, $p = 1, 2, \ldots, P$, placed in a frame of a fixed length consisting of both pilots and data symbols. During this step, to reduce the computational complexity, we assume that the channel coefficients at the consecutive time intervals are approximately equal to each other. The channel coefficients between each pair of transmit and receive antennas are then estimated by a pilot-aided LS estimation algorithm. In the next step, the fast fading channel coefficients are determined by an interpolation technique without assuming such an approximation as being constant over the consecutive estimation intervals. The variations in the fast fading channel are tracked in this way efficiently.

In Fig. 2, the frame structure is shown where the pilot symbols, employed for each pair of transmit antennas within each discrete-time duration n_p, $p = 0, 1, \ldots, P-1$, are inserted periodically in the time domain and the total number of pilots symbols placed in a block is B_p. Then, the received frames are operated for estimating the channel coefficients by the known pilot blocks at the pilot positions. Assuming that the channel transfer function is constant over two consecutive symbols, we can write the observation model as follows

$$\mathcal{Y}(n) = \mathcal{X}\mathcal{H}(n) + \mathcal{W}(n), \quad (8)$$

where $\mathcal{Y}(n) = \big[y_1(n) \quad y_2(n) \quad \cdots \quad y_{N_r}(n) \quad y_1(n+1) \quad y_2(n+1) \quad \cdots \quad y_{N_r}(n+1)\big]^{\mathrm{T}}$, $\mathcal{H}(n) = \big[h_{1,c_1}(n) \quad h_{2,c_1}(n) \quad \cdots \quad h_{N_r,c_1}(n) \quad h_{1,c_2}(n) \quad h_{2,c_2}(n) \quad \cdots \quad h_{N_r,c_2}(n)\big]^{\mathrm{T}}$, $\mathcal{W}(n) = \big[w_1(n) \quad w_2(n) \quad \cdots \quad w_{N_r}(n) \quad w_1(n+1) \quad w_2(n+1) \quad \cdots \quad w_{N_r}(n+1)\big]^{\mathrm{T}}$, $\mathcal{X} = \begin{bmatrix} \mathcal{X}_{p1} & \mathcal{X}_{p2} \\ -\mathcal{X}_{p2}^* & \mathcal{X}_{p1}^* \end{bmatrix}$,

$\mathcal{X}_{p1} = \mathrm{diag}[x_{p1} \quad x_{p1} \quad \cdots \quad x_{p1}]\psi_c$ and $\mathcal{X}_{p2} = \mathrm{diag}[x_{p2} \quad x_{p2} \quad \cdots \quad x_{p2}]\psi_c$.

From (8), the LS solution of the observation model for $(\mathcal{X}^{\dagger}\mathcal{X})^{-1} = (1/2E_{\mathrm{av}})$, where E_{av} is average symbol energy, can be expressed as

$$\widehat{\mathcal{H}}(n) = (1/2E_{\mathrm{av}})\mathcal{X}^{\dagger}\mathcal{Y}(n). \tag{9}$$

In this paper, a time-varying Rayleigh fading channel with a Doppler effect is considered. Therefore, the estimated channel coefficients in a block cannot be employed as the channel response of the next data block. Thus, variation of wireless radio channels in time makes dynamic estimation of such channels necessary [10]. The proposed CE technique in this paper is a promising one for the STBC-SM systems that dynamically estimates such channels. The coefficients of the time-varying CIR, in turn, are estimated at all data positions by a suitable interpolation technique, employing the pilot-aided estimated channel coefficients at the first step. The channel interpolation algorithms are discussed separately, in the following subsections.

4.1 Interpolation techniques

After estimation of the CIRs at pilot positions, channel coefficients at the positions of the unknown data symbols and the instances at which transmit antennas are not active can be determined by one of the suitable interpolation techniques. Consequently, $h_{\mathrm{r},j}(n_p)$, $j = 1, 2, \ldots, N_{\mathrm{t}}$, $r = 1, 2, \ldots, N_{\mathrm{r}}$ is estimated for $p = 0, 1, \ldots, P-1$ at the pilot positions while the channel variations at the data symbols should be estimated by an interpolation techniques.

4.1.1 Piecewise linear interpolation:

PLI is one of the most popular and frequently used interpolation techniques [11]. It can be expressed for $r = 1, 2, \ldots, N_{\mathrm{r}}$ and $p = 0, 1, 2, \ldots, P-1$ as follows

$$\begin{aligned} h_{\mathrm{r},j}(n) &= \hat{h}_{\mathrm{r},j}(n_p) + \left(\hat{h}_{\mathrm{r},j}(n_{p+1}) - \hat{h}_{\mathrm{r},j}(n_p)\right)\left(\frac{n-n_p}{D}\right), \\ &\text{for } j = c_1, c_2;\; n_p \le n \le n_{p+1} \end{aligned} \tag{10}$$

where $\hat{h}_{\mathrm{r},j}(n_p)$ is the estimated CIRs at pilot positions, D is the distance between two consecutive pilot symbols (i.e. $D = n_{p+1} - n_p$) and $h_{\mathrm{r},j}(n)$ denotes the estimated CIRs at all data positions. P is the total number of pilot symbols by which the LS estimated channel coefficients are obtained. The interval index p must be determined in such a way that $n_p \le n \le n_{p+1}$, in which the pilot symbols are located.

4.1.2 Piecewise cubic Hermite interpolation:

It is known that another effective way for the interpolation is the use of the piecewise cubic polynomials [12]. Consider the following function on the interval $n_p \le n \le n_{p+1}$, expressed in terms of the local variables $m = n - n_p$ and for $j = c_1, c_2$,

$$\begin{aligned} h_{\mathrm{r},j}(n) = \frac{3Dm^2 - 2m^3}{D^3}\hat{h}_{\mathrm{r},j}(n_{p+1}) + \frac{D^3 - 3Dm^2 + 2m^3}{D^3} \\ \hat{h}_{\mathrm{r},j}(n_p) + \frac{m^2(m-D)}{D^2}d_{p+1} + \frac{m(m-D)^2}{D^2}d_p \end{aligned} \tag{11}$$

where d_p is the slope of the interpolant at n_p. To obtain the piecewise cubic Hermite interpolation, we now describe the *pchip* and SI techniques in the following subsections below.

Shape-preserving piecewise cubic Interpolation (pchip): The PI, described in [13], guarantees that the interpolated value stays within the limits of the local data points. This interpolant determines the slopes d_p in such a way that the function values do not overshoot the data values. Let the first-order difference of $\hat{h}_{\mathrm{r},j}(n_p)$ be defined as

$$\delta_p = \frac{\hat{h}_{\mathrm{r},j}(n_{p+1}) - \hat{h}_{\mathrm{r},j}(n_p)}{D}. \tag{12}$$

Assuming two pilot intervals have the same length, we set $d_p = 0$ if δ_p and δ_{p-1} have opposite signs, or if neither of them is zero. In this case, n_p is a discrete local minimum or maximum. In contrary, if δ_p and δ_{p-1} have the same sign, then d_p can be evaluated as

$$d_p = \frac{2\delta_{p-1}\delta_p}{\delta_{p-1} + \delta_p}. \tag{13}$$

Spline interpolation: SI is a piecewise cubic Hermite interpolation function having a continuous second-order derivative, and satisfies the same interpolation constraints as the pchip [7]. All d_p values can be calculated as follows

$$\boldsymbol{Ad} = \boldsymbol{r} \tag{14}$$

where

$$\boldsymbol{A} = \begin{bmatrix} D & 2D & & & & \\ D & 4D & D & & & \\ & D & 4D & D & & \\ & & \ddots & \ddots & \ddots & \\ & & & D & 4D & D \\ & & & & D & 4D \end{bmatrix}$$

is a tridiagonal matrix of D and $\boldsymbol{d} = [d_0, d_1, \cdots, d_{P-1}]^{\mathrm{T}}$ is a vector of the unknown slopes, d_p. The right-hand side of (14) is $\boldsymbol{r} = 3[(5/6)D\delta_0 + (1/6)D\delta_1, D\delta_0 + D\delta_1, \cdots, D\delta_{P-3} + D\delta_{P-2}, (1/6)D\delta_{P-3} + (5/6)D\delta_{P-2}]^{\mathrm{T}}$.

4.1.3 Low-pass interpolation:

LPI is another technique for the CE [14]. In our work, the CIRs at pilots are estimated by the LS technique and those channel parameters at the positions of data symbols are initially set to zeros. Then, a raised-cosine type of low-pass filter is applied to the zero-inserted CIRs to determine the entire CIRs as follows: First, the low-pass interpolator inserts $D-1$ zeros between successive samples of the signal $\hat{h}_{\mathrm{r},j}(n_p)$ with a sampling rate of f_p, as

$$\tilde{h}_{\mathrm{r},j}(n) = \begin{cases} \hat{h}_{\mathrm{r},j}(n_p), & n = 0 : D : D(P-1) \\ 0, & \text{otherwise.} \end{cases} \tag{15}$$

Consequently, the sampling period of the intermediate signal, $\tilde{h}_{\mathrm{r},j}(n)$, is reduced to T_p/D or the sampling rate is increased to $\tilde{f}_p = Df_p$. After this operation, the intermediate signal is convolved with a unit impulse response $h(n)$ of the low-pass filter to obtain the interpolated signal $h_{\mathrm{r},j}(n)$ as follows

$$h_{\mathrm{r},j}(n) = \sum_{n_p=-\infty}^{\infty} h(n-n_p)\tilde{h}_{\mathrm{r},j}(n_p) \tag{16}$$

where $h(n)$ is designed as in [15] with a cutoff frequency, specified by $f_{\mathrm{c}} = \tilde{f}_p/2D = f_p/2$.

4.1.4 Nearest interpolation:

To determine the interpolated signal, $h_{\mathrm{r},j}(n)$'s determined by a NI which convolves the intermediate signal, $\tilde{h}_{\mathrm{r},j}(n)$, with a $h(n)$ as

$$h_{\mathrm{r},j}(n) = \sum_{n_p=-\infty}^{\infty} h(n-n_p)\tilde{h}_{\mathrm{r},j}(n_p) \tag{17}$$

where

$$h(n) = \begin{cases} 1, & 0 \le n \le D \\ 0, & \text{otherwise.} \end{cases} \tag{18}$$

As shown in Fig. 3, LPI is the best method to track the time variation of the channel since it perfectly tracks the fading channel. Actually, performance differences between interpolation methods depend on the mean square error (MSE) between the interpolated points and their original values. As observed from Fig. 3, the MSE performance of NI is the worst of all the methods and, in computer simulations section, we show that NI has a irreducible error floor.

5 Computational complexity

The computational complexity of the proposed CE algorithm depends critically on the relative number of pilot points and the number of data points to interpolate. A computationally simple technique to estimate the wireless channel is the NI. There is no computational complexity involved in the implementation of the NI, since it interpolates between sample points by holding each sample value until the next sampling instant. On the other hand, we demonstrate that the PLI is one of the low computational complexity techniques with superior BER performance as compared with the NI for the STBC-SM systems while the computational complexity of the PLI is slightly higher than that of the NI. Nevertheless, the BER performance of the PLI degrades in the presence of rapidly time-varying channels.

Some versions of the piecewise polynomial interpolations such as ‘pchip’ and ‘spline’ may also be used to estimate the wireless channel coefficients. The slopes are determined by solving the tridiagonal system of equations in (14). The tridiagonal matrix algorithm is an efficient way of solving tridiagonal matrix systems [16]. However, due to their oscillatory response, an additional complexity is introduced as compared with PLI techniques. Moreover, the BER performance of piecewise polynomial interpolations is significantly degraded due to the high order modulation format employed during the transmission.

The computational load of the LPI algorithm in (16) can be determined by the number of fast Fourier transform (FFT) operations and thus, the computational complexity of the LPI is quite feasible by using the FFT. Consequently, it is seen that the complexity of the LPI is much lower than that of the piecewise polynomial interpolation algorithms, and a little more than that of the linear and NI algorithms. Therefore, the proposed LPI is computationally efficient and is very attractive to be adopted for the STBC-SM systems. Some quantitative analysis of interpolation methods employed in this paper are given in [17, 18]. Based on the above discussions and our computer simulation results, we can firmly state that the LPI performs the best among all of the 1D interpolation methods for STBC-SM systems.

6 Performance of STBC-SM under imperfect CSI

In this section, we analytically evaluate the ABEP of the STBC-SM scheme in the presence of CE errors by means of the PEP calculation. Let us consider the following transmission model

$$\boldsymbol{Y} = \boldsymbol{X}\boldsymbol{H} + \boldsymbol{N} \tag{19}$$

where $\boldsymbol{X} \in \mathbb{C}^{2\times N_t}$ is the transmitted STBC-SM matrix, $\boldsymbol{H} \in \mathbb{C}^{N_t \times N_r}$ is the channel matrix representing the MIMO channel, and $\boldsymbol{Y} \in \mathbb{C}^{2\times N_r}$ and $\boldsymbol{N} \in \mathbb{C}^{2\times N_r}$ represent the received signal and noise matrices, respectively. The distribution of the elements of $\boldsymbol{H}$ and $\boldsymbol{N}$ are given as $\mathcal{CN}(0, 1)$ and $\mathcal{CN}(0, N_0)$, respectively. We assume the normalisation of $E\{\|\boldsymbol{X}\|_F^2\} = 2$.

In practical systems, the channel estimator at the receiver provides an estimate of the matrix of the channel coefficients as [19]

$$\tilde{\boldsymbol{H}} = \boldsymbol{H} + \boldsymbol{E} \tag{20}$$

where $\boldsymbol{E}$ represents the matrix of CE errors which is independent of $\boldsymbol{H}$ and its elements follow $\mathcal{CN}(0, \sigma_\varepsilon^2)$ distribution. Although the

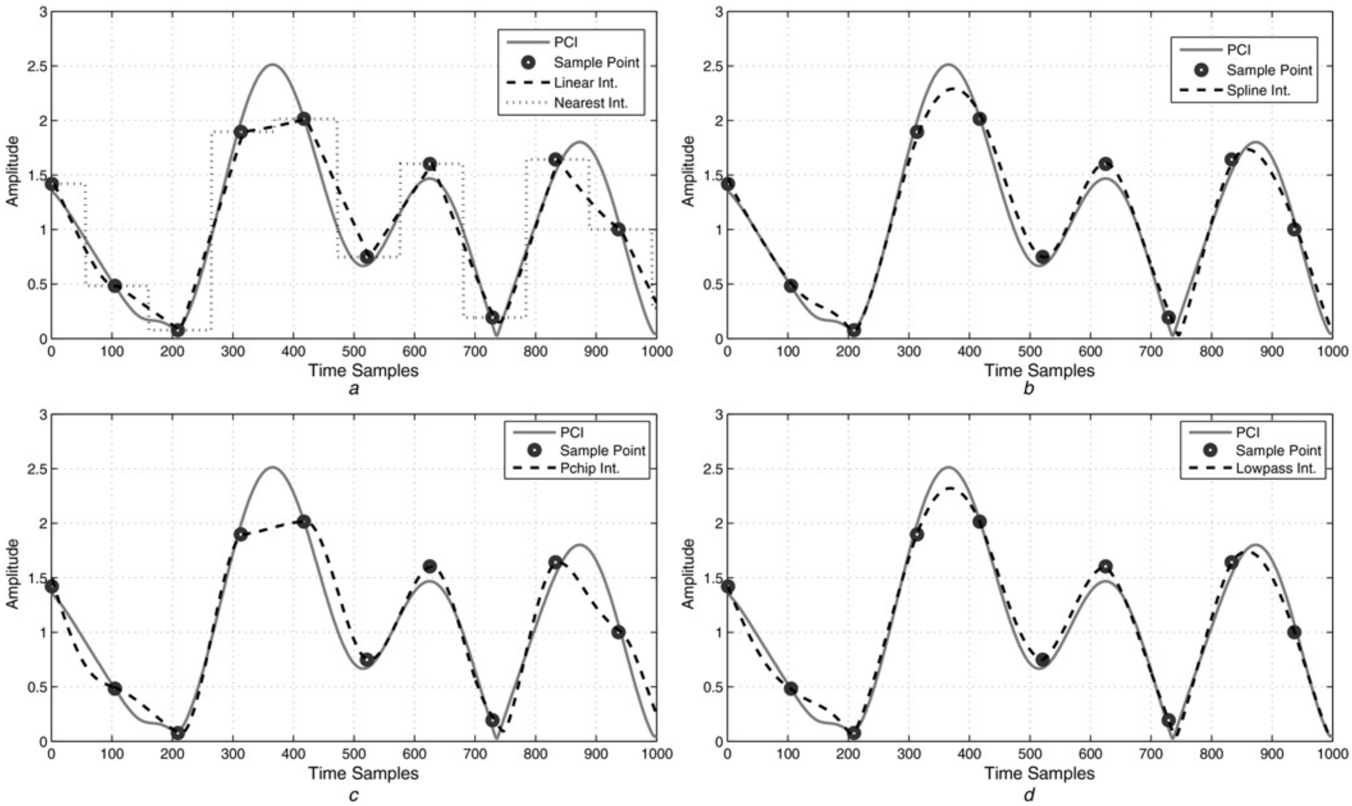

Fig. 3 *Time domain representation of interpolation methods with P-CSI*

IET Commun., 2016, Vol. 10, Iss. 14, pp. 1820–1828

model given in (20) is valid for the estimation of the channel coefficients using the LS method, it is widely used in the literature for the performance evaluation of systems with imperfect CSI. It is important to note that the elements of $\tilde{\boldsymbol{H}}$ are dependent of the elements of $\boldsymbol{H}$ with the correlation coefficient $\rho = 1/\sqrt{1+\sigma_\varepsilon^2}$, i.e. for $\sigma_\varepsilon^2 \to 0$, then $\rho \to 1$. The variance of the estimation error is adjusted in accordance with the noise power as $\sigma_\varepsilon^2 = N_0$, where one pilot is used in training per channel response sample.

Under CE errors, the receiver uses the mismatched ML decoder [20] by processing the received signal matrix given by (19) to detect the corresponding data matrix $\boldsymbol{X}$ as

$$\hat{\boldsymbol{X}} = \arg\min_{\boldsymbol{X}} \left\| \boldsymbol{Y} - \boldsymbol{X}\tilde{\boldsymbol{H}} \right\|_{\mathrm{F}}^2. \tag{21}$$

As seen from (21), the mismatched ML receiver uses the decision metric of the P-CSI case where $\boldsymbol{H}$ is replaced by $\tilde{\boldsymbol{H}}$. In order to calculate the conditional PEP (CPEP) of the STBC-SM scheme, which is defined as the probability of deciding to $\hat{\boldsymbol{X}}$ given that $\boldsymbol{X}$ is transmitted for a known $\tilde{\boldsymbol{H}}$ matrix, (19) should be rewritten in vector form as

$$\boldsymbol{y}_k = \boldsymbol{X}\boldsymbol{h}_k + \boldsymbol{n}_k, \quad k = 1, 2, \ldots, N_{\mathrm{r}} \tag{22}$$

where $\boldsymbol{y}_k$, $\boldsymbol{h}_k$ and $\boldsymbol{n}_k$ represent the kth columns of $\boldsymbol{Y}$, $\boldsymbol{H}$ and $\boldsymbol{N}$, respectively. Similarly, (20) can be rewritten as $\tilde{\boldsymbol{h}}_k = \boldsymbol{h}_k + \boldsymbol{e}_k$, where $\tilde{\boldsymbol{h}}_k$ and $\boldsymbol{e}_k$ represent the kth columns of $\tilde{\boldsymbol{H}}$, $\boldsymbol{E}$, respectively.

Considering (21) and (22), the CPEP of the STBC-SM scheme is calculated as

$$\begin{aligned} P\left(\boldsymbol{X}\to\hat{\boldsymbol{X}}|\tilde{\boldsymbol{H}}\right) &= P\left(\sum_{k=1}^{N_{\mathrm{r}}} \left\|\boldsymbol{y}_k - \boldsymbol{X}\tilde{\boldsymbol{h}}_k\right\|^2 > \sum_{k=1}^{N_{\mathrm{r}}} \left\|\boldsymbol{y}_k - \hat{\boldsymbol{X}}\tilde{\boldsymbol{h}}_k\right\|^2\right) \\ &= P\left(\sum_{k=1}^{N_r} \left\|\boldsymbol{X}\tilde{\boldsymbol{h}}_k\right\|^2 - \left\|\hat{\boldsymbol{X}}\tilde{\boldsymbol{h}}_k\right\|^2 - 2\Re\left\{\boldsymbol{y}_k^{\mathrm{H}}\left(\boldsymbol{X}-\hat{\boldsymbol{X}}\right)\tilde{\boldsymbol{h}}_k\right\} > 0\right) \\ &= P(G > 0) \end{aligned} \tag{23}$$

In (23), G is a Gaussian distributed random variable whose parameters can be calculated as follows. Conditioned on $\tilde{\boldsymbol{h}}_k$, the mean and the covariance matrix of $\boldsymbol{h}_k$ are calculated as $\rho^2\tilde{\boldsymbol{h}}_k$ and $\left(1-\rho^2\right)\boldsymbol{I}_{N_{\mathrm{t}}}$, respectively [20]. Therefore, considering the conditional mean and covariance matrix of $\boldsymbol{h}_k$, the conditional mean and the covariance matrix of $\boldsymbol{y}_k$ can be derived from (22) as $\rho^2\boldsymbol{X}\tilde{\boldsymbol{h}}_k$ and $\boldsymbol{X}\boldsymbol{X}^{\mathrm{H}}\left(1-\rho^2\right)+N_0\boldsymbol{I}_2$, respectively. Due to the orthogonality of the Alamouti's code employed in STBC-SM scheme, the covariance matrix of $\boldsymbol{y}_k$ simplifies to $\left(z\left(1-\rho^2\right)+N_0\right)\boldsymbol{I}_2$, where $z\boldsymbol{I}_2 = \boldsymbol{X}\boldsymbol{X}^{\mathrm{H}}$, i.e. $z = (1/2)\|\boldsymbol{X}\|_{\mathrm{F}}^2$, and for a constant envelope constellation such as M-PSK we obtain $z = 1$. Considering the conditional statistics of $\boldsymbol{y}_k$, the mean and the variance of the decision variable G are obtained, respectively, as follows after some algebra

$$E\{G\} = \sum_{k=1}^{N_{\mathrm{r}}} \left(1-2\rho^2\right)\left\|\boldsymbol{X}\tilde{\boldsymbol{h}}_k\right\|^2 - \left\|\hat{\boldsymbol{X}}\tilde{\boldsymbol{h}}_k\right\|^2 + 2\rho^2\Re\left\{\tilde{\boldsymbol{h}}_k^{\mathrm{H}}\boldsymbol{X}^{\mathrm{H}}\hat{\boldsymbol{X}}\tilde{\boldsymbol{h}}_k\right\} \tag{24}$$

$$\mathrm{Var}\{G\} = 2\left(z\left(1-\rho^2\right)+N_0\right)\left\|\left(\boldsymbol{X}-\hat{\boldsymbol{X}}\right)\tilde{\boldsymbol{H}}\right\|_{\mathrm{F}}^2. \tag{25}$$

Defining $\tilde{G} = \rho^2 G$ and assuming $\rho^2 \simeq \rho^4$, which is quite reasonable for high SNR values, we obtain

$$E\{\tilde{G}\} \simeq -\rho^2\left\|\left(\boldsymbol{X}-\hat{\boldsymbol{X}}\right)\tilde{\boldsymbol{H}}\right\|_{\mathrm{F}}^2 \tag{26}$$

$$\mathrm{Var}\{\tilde{G}\} = 2\rho^4\left(z\left(1-\rho^2\right)+N_0\right)\left\|\left(\boldsymbol{X}-\hat{\boldsymbol{X}}\right)\tilde{\boldsymbol{H}}\right\|_{\mathrm{F}}^2. \tag{27}$$

Finally, the CPEP of the STBC-SM scheme obtained from (27) as

$$P\left(\boldsymbol{X}\to\hat{\boldsymbol{X}}|\tilde{\boldsymbol{H}}\right) \simeq Q\left(\sqrt{\frac{\left\|\left(\boldsymbol{X}-\hat{\boldsymbol{X}}\right)\tilde{\boldsymbol{H}}\right\|_{\mathrm{F}}^2}{2\left(z\left(1-\rho^2\right)+N_0\right)}}\right). \tag{28}$$

Using alternative form of the Q function [21], (28) can be rewritten as

$$P\left(\boldsymbol{X}\to\hat{\boldsymbol{X}}|\tilde{\boldsymbol{H}}\right) \simeq \frac{1}{\pi}\int_0^{\pi/2} \exp\left(-\frac{\Gamma}{2\Delta\sin^2\theta}\right)\mathrm{d}\theta \tag{29}$$

where $\Gamma = \left\|\left(\boldsymbol{X}-\hat{\boldsymbol{X}}\right)\tilde{\boldsymbol{H}}\right\|_{\mathrm{F}}^2$ and $\Delta = 2(z(1-\rho^2)+N_0)$. In order to obtain unconditional PEP (UPEP) of the STBC-SM system, (29) should be averaged over $p_\Gamma(\Gamma)$ as

$$P\left(\boldsymbol{X}\to\hat{\boldsymbol{X}}\right) \simeq \frac{1}{\pi}\int_0^\infty\int_0^{\pi/2} \exp\left(-\frac{\Gamma}{2\Delta\sin^2\theta}\right)p_\Gamma(\Gamma)\,\mathrm{d}\theta\,\mathrm{d}\Gamma \tag{30}$$

which results

$$P\left(\boldsymbol{X}\to\hat{\boldsymbol{X}}\right) \simeq \frac{1}{\pi}\int_0^{\pi/2} M_\Gamma\left(\frac{-1}{2\Delta\sin^2\theta}\right)\mathrm{d}\theta. \tag{31}$$

To find the MGF of Γ, it should be expressed in quadratic form as $\Gamma = \sum_{k=1}^{N_{\mathrm{r}}}\tilde{\boldsymbol{h}}_k^{\mathrm{H}}\boldsymbol{Q}\tilde{\boldsymbol{h}}_k$ where $\boldsymbol{Q} = \left(\boldsymbol{X}-\hat{\boldsymbol{X}}\right)^{\mathrm{H}}\left(\boldsymbol{X}-\hat{\boldsymbol{X}}\right)$. Defining the covariance matrix of $\tilde{\boldsymbol{h}}_k$ as $\boldsymbol{L} = E\left\{\tilde{\boldsymbol{h}}_k\tilde{\boldsymbol{h}}_k^{\mathrm{H}}\right\} = \left(1+\sigma_\varepsilon^2\right)\boldsymbol{I}_{N_{\mathrm{t}}}$, the MGF of Γ is obtained from [22] as

$$M_\Gamma(t) = \left[\det\left(\boldsymbol{I}_{N_{\mathrm{t}}} - t\boldsymbol{L}\boldsymbol{Q}\right)\right]^{-N_{\mathrm{r}}} \tag{32}$$

since $\tilde{\boldsymbol{h}}_k$'s are independent and identically distributed. Considering the eigenvalues of $\boldsymbol{Q}$, which are defined as λ_i, $i = 1, \ldots, R$, where $R = \mathrm{rank}(\boldsymbol{Q})$, (32) can be further simplified as

$$M_\Gamma(t) = \left[\prod_{i=1}^{R}\left(1 - t\left(1+\sigma_\varepsilon^2\right)\lambda_i\right)\right]^{-N_{\mathrm{r}}}. \tag{33}$$

Finally, combining (31) and (33), the UPEP of the STBC-SM scheme is obtained as

$$P\left(\boldsymbol{X}\to\hat{\boldsymbol{X}}\right) \simeq \frac{1}{\pi}\int_0^{\pi/2}\left[\prod_{i=1}^{R}\left(1+\frac{\left(1+\sigma_\varepsilon^2\right)\lambda_i}{2\Delta\sin^2\theta}\right)\right]^{-N_{\mathrm{r}}}\mathrm{d}\theta. \tag{34}$$

A closed form expression can be found for the integral in (34) using the general formulas given [21].

Remark 1: It is known that the diversity order of the STBC-SM system is equal to $R = 2$, which is the rank of the distance matrix $\boldsymbol{Q}$ [4]. Therefore, (34) is simplified as

$$P\left(\boldsymbol{X}\to\hat{\boldsymbol{X}}\right) \simeq \frac{1}{\pi}\int_0^{\pi/2}\left(1+\frac{\left(1+\sigma_\varepsilon^2\right)\lambda_1}{2\Delta\sin^2\theta}\right)^{-N_r}\left(1+\frac{\left(1+\sigma_\varepsilon^2\right)\lambda_2}{2\Delta\sin^2\theta}\right)^{-N_{\mathrm{r}}}\mathrm{d}\theta \tag{35}$$

which has a closed from solution in (5A.58) of [21].

Remark 2: Please note that setting $\sigma_\varepsilon^2 = 0$ $(\rho = 1)$ in (35) yields

$$P\left(\boldsymbol{X}\to\hat{\boldsymbol{X}}\right) = \frac{1}{\pi}\int_0^{\pi/2}\left(1+\frac{\lambda_1}{4N_0\sin^2\theta}\right)^{-N_{\mathrm{r}}}\left(1+\frac{\lambda_2}{4N_0\sin^2\theta}\right)^{-N_{\mathrm{r}}}\mathrm{d}\theta \tag{36}$$

which is the UPEP of the STBC-SM for the P-CSI case given in (22) of [4].

After the evaluation UPEP, an approximation (not necessarily an upper bound since the UPEP of (36) is an approximated one) on the ABEP of the STBC-SM scheme can be obtained as

$$P_{\mathrm{b}} \simeq \frac{1}{vn_X} \sum_{X} \sum_{\hat{X}} P(\boldsymbol{X} \to \hat{\boldsymbol{X}}) e(\boldsymbol{X} \to \hat{\boldsymbol{X}}) \tag{37}$$

where v is the total number of information bits transmitted per $\boldsymbol{X}$, n_X is the number of the possible realisations of $\boldsymbol{X}$ and $e(\boldsymbol{X} \to \hat{\boldsymbol{X}})$ represents the number of bit errors for the corresponding pairwise error event $(\boldsymbol{X} \to \hat{\boldsymbol{X}})$.

7 Simulation results

The BER performance of STBC-SM systems is evaluated by Monte Carlo simulations employing QPSK, 16-QAM and 64-QAM signal constellations. The sampling frequency is chosen as 0.1 MHz. A single 4×4 STBC-SM block consists of $B_p + D = 104$ samples with $B_p = 4$ pilot symbols. Totally, 10 blocks are transmitted in a frame (i.e. one frame consists of $N = 10(B_p + D)$ samples). The SNR is defined as E_s/N_0 where E_s is signal energy per symbol and N_0 is noise power spectral density. In our computer simulations, the mobile terminal is moving with a speed of a 150 km/h with carrier frequency equal to 1.8 GHz.

In Fig. 4*a*, BER performance of the proposed interpolation techniques are compared for the QPSK signalling. It is observed that the LPI outperforms slightly the pchip and PLI while it has similar performance to the SI. The pchip and the PLI have similar BER performances but they perform better than the NI. It is also demonstrated that the NI has an irreducible error floor at high SNR and mobility values.

Since the large bandwidth efficiency is one of the main goals to achieve in mobile wireless communications systems, the performance of the higher order modulations schemes such as 16-QAM and 64-QAM is also considered in Figs. 4*b* and *c*. In [23], it has been shown that the QAM is very sensitive to CE errors and the performance degradation of a higher order QAM scheme is more serious than that of the lower order QAM. The effect of CE on the BER performance for 16-QAM is presented in Fig. 4*b*. In particularly, it is seen from Fig. 4*b* that the LPI exhibits a detection gain of about 1.5 and 2.5 dB over the PI and the PLI at a BER value of 10^{-6}, respectively.

BER performance results of the aforementioned interpolation algorithms, for 64-QAM, are plotted in Fig. 4*c* a function of the SNR. As can be seen from Fig. 4*c*, the BER performance of the CE algorithm based on the LPI is substantially better than that of all the

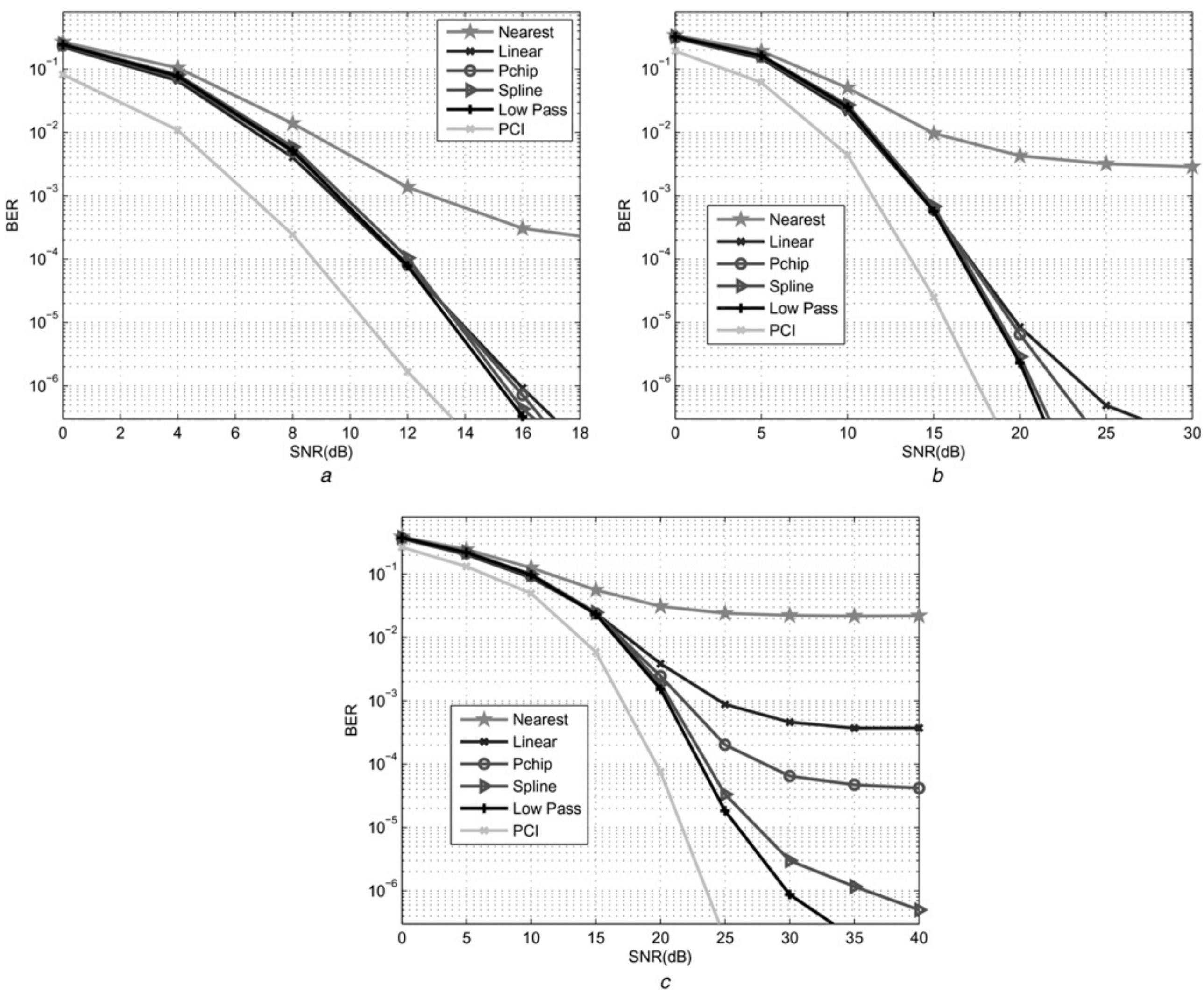

Fig. 4 *BER performance of 4 × 4*

a QPSK-STBC-SM
b 16QAM-STBC-SM
c 64QAM-STBC-SM with PA-CE

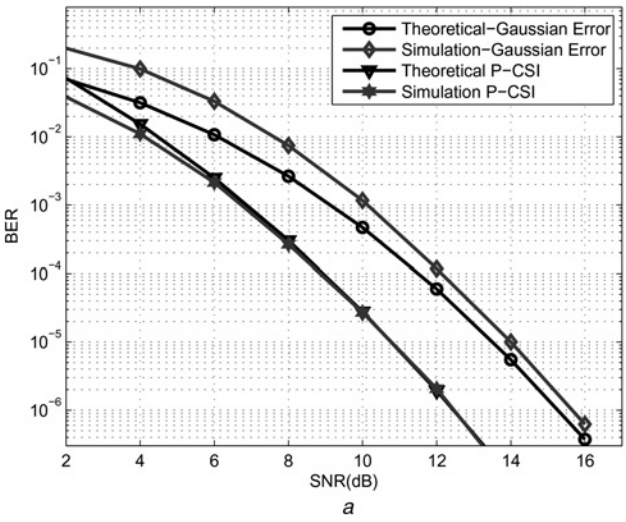

Fig. 5 *BER performance of QPSK-STBC-SM*

a With/without CE
b For Low-pass interpolator

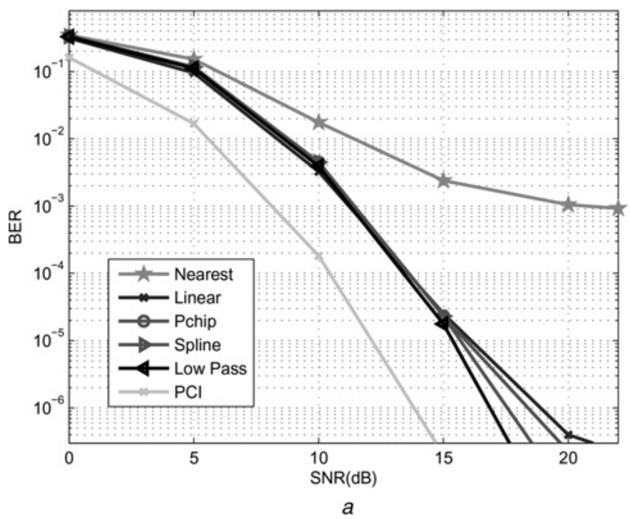

Fig. 6 *BER performance of 8 × 4*

a QPSK-STBC-SM
b 16QAM-STBC-SM with PA-CE

proposed interpolation algorithms while it also experiences performance degradation at higher SNR values. As can be also observed from Fig. 4*c*, particularly the BER performances of the NI, PLI and the PI are significantly degraded due to the higher order modulation type. Based on the above discussions and the observations, it is concluded that the SNR gain of the LPI is increased significantly relative to other interpolation techniques for high order QAM constellations. For instance, it is demonstrated that the LPI exhibits a detection gain of about 5 dB over the SI at a BER value of 10^{-6}.

In Fig. 5*a*, theoretical BER performance results of the STBC-SM are shown and compared with the computer simulation results obtained for the P-CSI case. It is shown that the theoretical curve is very close to the computer simulation results. As seen from Fig. 5*a*, the theoretical curve is still very tight with increasing SNR values under the imperfect CE scenario. Moreover, the derived curve of the STBC-SM is also compared with the low-pass interpolated technique in Fig. 5*b* where the MSE of the low-pass interpolated technique is calculated and used in the derived theoretical expression. It is shown that error probability curves of the proposed CE technique approach to the theoretical curve at higher SNR values.

7.1 Investigation of total number of pilots and higher number of transmit antennas

We also investigated the performance of a different MIMO system configuration such as 8×4 by computer simulations. As can be seen from Fig. 6, for QPSK and 16-QAM signalling, BER performance of the LPI is better than that of all the proposed interpolation algorithms. In particular, it is seen from Fig. 6*b* that the LPI exhibits a detection gain of about 1 and 4.1 dB over the SI and the PLI at a BER value of 10^{-6}, respectively.

In real applications, a low percentage of the pilots is desired since the large number of inserted pilots reduce the spectral efficiency of the overall system. On the other hand, the placement of pilots in the data stream becomes more critical for fast time varying communications systems in designing high quality algorithms to track the channel variations. Thus, we also investigated the performance of CE methods for different pilot insertion rates presented in Fig. 7*a* for 64-QAM at SNR = 30 dB. It is seen from Fig. 7*a* that the pilot distances are 100, 96, 73 and 66 for the LPI, SI, PI and PLI at a BER value of 10^{-6}, respectively. It can be concluded from Fig. 7*a* that the LPI based CE

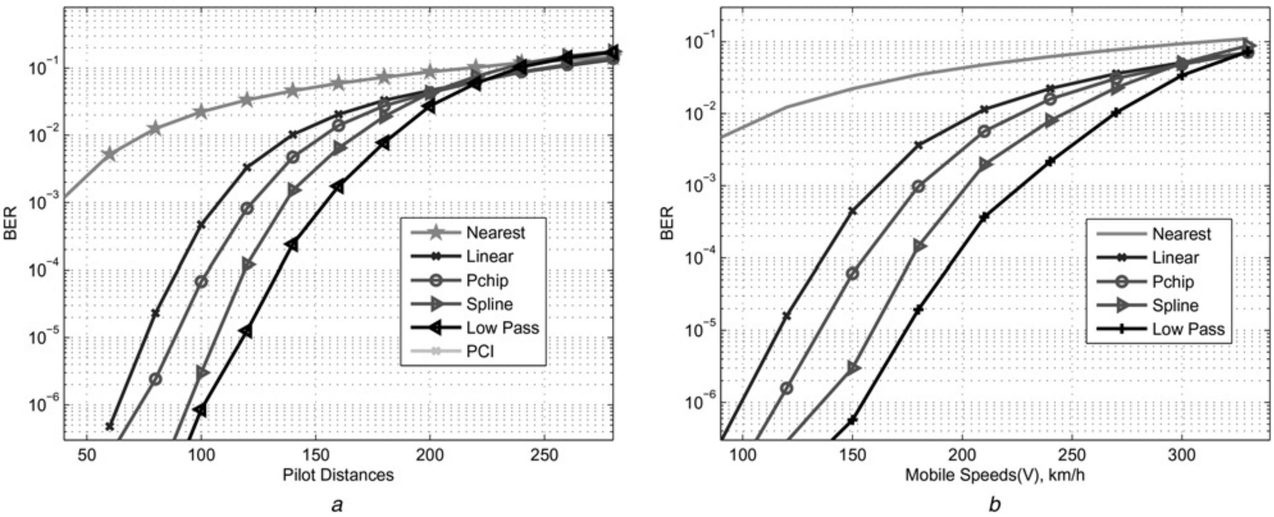

Fig. 7 *BER performance of 4 × 4 64QAM-STBC-SM at SNR = 30 dB for*
a Different pilot space
b Different velocity

require less pilots; therefore it has more bandwidth efficiency than that of all the proposed interpolation algorithms.

Mobility support is one of the key features of new generation wireless systems. To show that the proposed CE, is robust to different mobility levels, we investigated the effect of the velocity on the BER performance of the proposed interpolation techniques, as shown in Fig. 7*b* for 64-QAM at SNR = 30 dB. As can be seen from Fig. 7*b*, the proposed LPI is more robust to mobility than that of all the other interpolation algorithms.

Consequently, the performance improvement of the LPI, in the case of the high mobility, less number of pilots, large number of antennas and higher order modulations, indicates that it is a better choice for an STBC-SM system which can be considered in the future standards and to meet the expectations of the next-generation wireless communications systems.

8 Conclusions

In this paper, we proposed a novel CE method based on interpolation in the presence of rapidly varying wireless channels for STBC-SM systems. In order to detect the STBC-SM signal coherently, an accurate channel estimate is essential. One of the important conclusions of this paper is that the performance of an STBC-SM system can be remarkably affected by the channel estimation performance. Consequently, in the design of the future wireless communications systems, developing low complexity and efficient CE algorithms, compatible with STBC-SM schemes, would be the most important task to be implemented at the receivers.

It has been shown that the PA-CE with LPI technique performs the best among all the CE techniques since it allows tracking the fading channel very efficiently as the MSE between the interpolated points and their original values is minimised. On the other hand, the low complexity PLI schemes could also be employed when more pilot symbols are allowed to use or the channel is a slowly time-varying type. Moreover, the CE error performance has been studied through the approximate ABEP of the STBC-SM. The theoretical ABEP has been shown to become very tight with the computer simulation results as the SNR increases and the performance of the proposed CE technique approaches to that of the one obtained by theoretical methods.

9 Acknowledgments

This work was supported in part by the Turkish Scientific and Technical Research Institute (TUBITAK) under grant no. 114E011. This work was also supported in part by the Research Fund of the University of Istanbul, project nos. 44182 and 45861.

10 References

1 Sanayei, S., Nosratinia, A.: 'Antenna selection in MIMO systems', *IEEE Commun. Mag.*, 2004, **42**, (10), pp. 68–73
2 Mesleh, R., Haas, H., Ahn, W., *et al.*: 'Spatial modulation-a new low complexity spectral efficiency enhancing technique'. IEEE First Int. Conf. on Communications and Networking in China 2006, October 2006, pp. 1–5
3 Alamouti, S.M.: 'A simple transmit diversity technique for wireless communications', *IEEE J. Sel. Areas Commun.*, 1998, **16**, (8), pp. 1451–1458
4 Başar, E., Aygölü, Ü., Panayırcı, E., *et al.*: 'Space-time block coded spatial modulation', *IEEE Trans. Commun.*, 2011, **59**, (3), pp. 823–832
5 Andrews, G., Ghosh, A., Muhamed, R.: 'Fundamentals of WiMAX: understanding Broadband Wireless Networking' (Pearson Education, 2007)
6 Dahlman, E., Parkvall, S., Skold, J.: '4G: LTE/LTE-advanced for mobile broadband' (Academic Press, 2013)
7 Coleri, S., Ergen, M., Puri, A., *et al.*: 'Channel estimation techniques based on pilot arrangement in OFDM systems', *IEEE Trans. Broadcast.*, 2002, **48**, (3), pp. 223–229
8 Le, T., Ngo, D., Mai, A., *et al.*: 'High-rate space-time block coded spatial modulation'. IEEE Int. Conf. on Advanced Technologies for Communications, October 2012, pp. 278–282
9 Li, X., Wang, L.: 'High rate STBC spatial modulation with cyclic structure', *IEEE Commun. Lett.*, 2014, **18**, (4), pp. 532–535
10 Bahai, R., Saltzberg, R., Ergen, M.: 'Multi-carrier digital communications: theory and applications of OFDM' (Springer Science & Business Media, 2004)
11 Hsieh, H., Wei, H.: 'Channel estimation for OFDM systems based on comb-type pilot arrangement in frequency selective fading channels', *IEEE Trans. Consum. Electron.*, 1998, **44**, (1), pp. 217–225
12 Dyer, A., Dyer, S.: 'Cubic-spline interpolation. 1', *IEEE Instrum. Meas. Mag.*, 2001, **4**, (1), pp. 44–46
13 Kahaner, D., Moler, C., Nash, S.: 'Numerical methods and software' (Prentice Hall, Englewood Cliffs, 1989)
14 Colieri, S., Ergen, M., Puri, A., *et al.*: 'A study of channel estimation in OFDM systems'. Vehicular Technology Conf. Proc. 56th IEEE VTC, 2002, vol 2, pp. 894–898
15 IEEE Acoustics, Speech, Signal Processing Society. DSP Committee: 'Programs for digital signal processing' (IEEE Press, 1979)
16 Conte, D., Boor, D.: 'Elementary numerical analysis: an algorithmic approach' (McGraw-Hill Higher Education, 1980)
17 Lehmann, T.M., Claudia, G., Klaus, S.: 'Survey: Interpolation methods in medical image processing', *IEEE Trans. Med. Imaging*, 1999, **18**, (11), pp. 1049–1075
18 Toraichi, K., Katagishi, K., Sekita, I., *et al.*: 'Computational complexity of spline interpolation', *Int. J. Syst. Sci.*, 1987, **18**, (5), pp. 945–954
19 Tarokh, V., Seshadri, N., Calderbank, R.: 'Space-time codes for high data rate wireless communication: Performance criterion and code construction', *IEEE Trans. Inf. Theory*, 1998, **44**, (2), pp. 744–765
20 Taricco, G., Biglieri, E.: 'Space-time decoding with imperfect channel estimation', *IEEE Trans. Wirel. Commun.*, 2005, **4**, (4), pp. 1874–1888
21 Simon, M.K., Alouini, S.: 'Digital communication over fading channels' (John Wiley & Sons, 2005)
22 Turin, L.: 'The characteristic function of Hermitian quadratic forms in complex normal variables', *Biometrika*, 1960, **47**, (1–2), pp. 199–201
23 Xia, B., Wang, J.: 'Effect of channel-estimation error on QAM systems with antenna diversity', *IEEE Trans. Commun.*, 2005, **53**, (3), pp. 481–488